Mathematical Modeling and Stability Analysis of Covid-19 Transmission Dynamics

S. I. Nwakaego[1], Prof. G. C. E. Mbah[2],
[1]*University of Delta, Agbor, Delta State, Nigeria*
[2]*University of Nigeria, Nsukka. Enugu State, Nigeria*

***Abstract*—Coronavirus Disease 2019 (COVID-19) emerged as a global pandemic with significant health and economic impacts. Mathematical modeling provides a quantitative tool for understanding disease transmission and evaluating control strategies. This study formulated and analyzed a deterministic SEIR model for COVID-19 transmission dynamics and applied optimal control theory to determine cost-effective intervention strategies. The model was analyzed for existence and stability of equilibrium points, and the basic reproduction number R_0 was derived using the next-generation matrix method.**

Stability analysis showed that the disease-free equilibrium is globally asymptotically stable when $R_0 < 1$, while the endemic equilibrium is stable when $R_0 > 1$. Sensitivity analysis identified the transmission rate and recovery rate as the most influential parameters on R_0.

To minimize the burden of exposed and infectious individuals, three time-dependent controls were introduced: prevention to reduce transmission, treatment to increase recovery, and awareness to reduce progression from exposed to infectious class. Pontryagin's Maximum Principle was used to characterize the optimal controls, and the optimality system was solved numerically using the forward-backward sweep method.

Numerical simulations revealed that all controls should be applied maximally at the onset of the epidemic and gradually reduced as the disease declines. Prevention control had the greatest effect on reducing transmission. The combined optimal control strategy significantly lowered the peak of infection and achieved disease elimination faster compared to the no-control scenario.

The results of this study provide theoretical guidance for public health policymakers on the timing and intensity of interventions needed to control COVID-19 outbreaks in a cost-effective manner.

***Index Terms*—COVID-19, SEIR model, Basic reproduction number, Stability analysis, Sensitivity Analysis,**

I. INTRODUCTION

The emergence of severe acute respiratory syndrome corona virus 2(SARS-CoV-2) in late 2019 led to the global COVID-19 pandemic, characterized by rapid human-to-human transmission and substantial morbidity and mortality. Despite vaccine rollout and public health measures, COVID-19 remains endemic in many regions, with new variants and waning immunity complicating control efforts. Mathematical models provide a quantitative framework to predict disease spread, evaluate intervention strategies and inform policy decisions.[2] Compartmental models based on system of ordinary differential equations are widely used to study COVID-19 dynamics. However, for any epidemiological model to be biological meaningful, solutions must remain positive and bounded within a feasible region for all $t \geq 0$. establishing positivity and invariance is therefore a necessary first step in model analysis. Understanding long term-term behavior requires equilibrium analysis. the disease-free equilibrium (DFE)represents a state where infection is absent, while the endemic equilibrium (EE)corresponds to persistent infection. The transition between these states is governed by the basic reproduction number, Ro. Ro is defined as the average number of secondary infections produced by a single infected individual in a fully susceptible population. Ro is typically computed using the next generation matrix method and acts as a threshold parameter. Not all parameters contribute equally to Ro. Sensitive analysis quantifies how changes in model parameters affect Ro, allowing identification of key drivers of transmission. This is critical for prioritizing cost-effective interventions such as reducing contact rate, improving treatment, or increasing vaccination. The stability properties of

equilibria determine whether the disease will die out or persist. Stability analysis using linearization, Routh-Hurwitz criteria, and Lyapunov functions establishes conditions under which the DFE or EE is locally and globally asymptotically stable. These results link directly to Ro and provide theoretical justification for control measures.

Despite progress, challenges remain in quantifying the effect of multiple controls like vaccination and treatment simultaneously. Optimal control theory provides a framework to determine time-dependent strategies that minimize infections while keeping costs low [Lenhart and Workman].

The objective of this paper is to perform a comprehensive stability analysis of a COVID-19 transmission model in a human population. SPECIFICALLY, we (1) prove positivity and invariance of solutions, (2) determine and analyze equilibria, (3) compute the basic reproduction number R_O and (4) establish stability conditions for both disease-free and endemic states, and perform sensitivity analysis. 4. Analyze local and global stability of equilibria 'and numerical Simulation results. The findings contribute to understanding COVID-19 dynamics and support evidence-based public health strategies.

II. THE SEIRTV MODEL

2.1. Model Formulation and Analysis

This section presents the formulation of a deterministic modified SEIR model for COVID-19 transmission dynamics. The model incorporates the flow of individuals from the susceptible to exposed, then infectious, and finally Recovered. We state the assumptions underlying the model, derive the system of differential equations, and analyze basic properties such as positivity and boundedness of solutions. The disease-free and endemic equilibrium points are determined, and the basic reproduction number Ro is computed using the next-generation matrix method. Finally, local and global stability of equilibria are analyzed, followed by sensitive analysis to identify parameters that most influence disease spread.

2.2 Model Assumptions

To formulate the model, the following assumptions are made based on epidemiological knowledge of COVID-19 and standard SEIRTV modelling practice:

1. The total population N(t) is divided into six mutually exclusive compartments:
   Susceptible S(t), Exposed E(t), infectious I(t), Recovered R(t), Treatment T(t) and Vaccination V(t) such that $N(t) = S(t) + E(t) + I(t) + R(t) + T(t) + V(t)$ is dynamic with birth rate Λ and natural death μ.
2. Only susceptible individuals S can be vaccinated at a rate $u_1(t)$. Vaccine efficacy is $1 - \sigma$, where σ is vaccine failure rate.
3. Exposed individuals E are infected but not infectious. They progress to infected class I at a rate α.
4. Infected individuals I can recover naturally at a rate γ_1 or receive treatment at control rate $u_2(t)$ and move to treat class T.
5. Treated individuals T recover at rate γ_2 and may experience disease-induced death rate δ.
6. Recovered individuals R gain temporary immunity but can lose it and return to S at a rate ω.
7. Vaccinated individuals V can wane back to S at a rate θ.
8. Disease-induced death occurs only in I and T classes.

2.3. Model Equations

The model equations are:

$$\frac{dS}{dt} = \Lambda - \mu S - \beta \frac{SI}{N} - \omega S$$

$$\frac{dE}{dt} = \beta \frac{SI}{N} - (\sigma + \mu)E$$

$$\frac{dI}{dt} = \sigma E - (\gamma + \delta + \theta + \mu)I$$

$$\frac{dR}{dt} = \gamma I + \alpha T - \mu R$$

$$\frac{dT}{dt} = \theta I - (\alpha + \mu)T$$

$$\frac{dV}{dt} = \omega S - \mu V$$

Where we let S(t), E(t), I(t), T(t) R(t), V(t) be Susceptible, Exposed, Infected, Treated, Recovered, and vaccinated respectively.

Force of infection is $\lambda(t) = \frac{\beta I(t)}{N(t)}$ where β is the transmission rate.

With two conditions $u_1(t)$ is the vaccination rate, $u_2(t)$ is the treatment rate, $0 \leq u_1(t) \leq 1$:

$$\frac{dS}{dt} = \Lambda + \omega R + \theta V - \lambda S - (\mu + u_1)S.$$

$N(t) = S + E + I + T + R + V$

$\frac{dN}{dt} = \frac{d}{dt} + \frac{dE}{dt} + \frac{dI}{dt} + \frac{dT}{dt} + \frac{dR}{dt} + \frac{dV}{dt}$.

Little Algebra gives $\frac{dN}{dt} = \Lambda - \mu N - \delta(I + T)$.

2.4. Positivity and Invariant Region

Theorem 1: Positivity

For non-negative initial conditions S(O), E(O), I(O), T(O) R(O), V(O)≥ $0, the\ solutions\ of\ the\ system\ remain\ non-negative$ for all t> 0.

Proof. From

$\left.\frac{dS}{dt}\right|_{S=0} = \Lambda + \omega R + \theta V \geq 0,$

and similarly for the other compartments, the positive orthant $\mathbb{R}^6_+$ is invariant. ▫

Invariant Region. Let

$\Gamma = \left\{(S, E, I, T, R, V) \in \mathbb{R}^6_+ : N \leq \frac{\Lambda}{\mu}\right\}$.

From

$\frac{dN}{dt} = \Lambda - \mu N - \delta(I + T) \leq \Lambda - \mu N,$

we find

$N(t) \leq N(0)e^{-\mu t} + \frac{\Lambda}{\mu}(1 - e^{-\mu t})$.

Thus

$\limsup_{t\to\infty} N(t) \leq \frac{\Lambda}{\mu}$.

Hence Γ is positively invariant and all solutions starting in Γ remain there.

2.5. Equilibrium Analysis and Computation of R_O.

Disease-free Equilibrium DFE

$E^O = (S^O, 0,0,0,0,V^0)$

where

$S^O = \frac{\Lambda(\theta+\mu)}{\mu(\theta+\mu+u_1)}$, $V^O = \frac{\Lambda u_1}{\mu(\theta+\mu+u_1\}}$,

Endemic Equilibrium: Endemic Equilibrium exists when $R_O > 1$. We set RHS of all model equations = 0 and solve for $I^* > 0$.

Basic Reproduction Number R_0.

Using next generation matrix method on the infected compartments E and I, the new-infection matrix is

$\mathcal{F} = \begin{pmatrix} 0 & \frac{\beta S^0}{N^0} + \frac{\sigma\beta V^0}{N^0} \\ 0 & 0 \end{pmatrix}$,

and the transition matrix is

$\mathcal{V} = \begin{pmatrix} \alpha + \mu & 0 \\ -\alpha & \gamma_1 + \delta + \mu + u_2 \end{pmatrix}$.

Then

$R_0 = \rho(\mathcal{F}\mathcal{V}^{-1}) = \frac{\beta\alpha\,(S^0 + \sigma V^0)}{N^0(\alpha+\mu)(\gamma_1+\delta+\mu+u_2)}$.

At the DFE, $N^0 = S^0 + V^0$, so

$R_0 = \frac{\beta\alpha}{(\alpha+\mu)(\gamma_1+\delta+\mu+u_2)} \cdot \frac{S^0 + \sigma V^0}{S^0 + V^0}$.

When $R_0 < 1$ the disease dies out, and if $R_0 > 1$ the disease persists (endemic).

The flow diagram of the SEIRTV model is illustrated as follows

Flow Diagram3. Flow Diagram

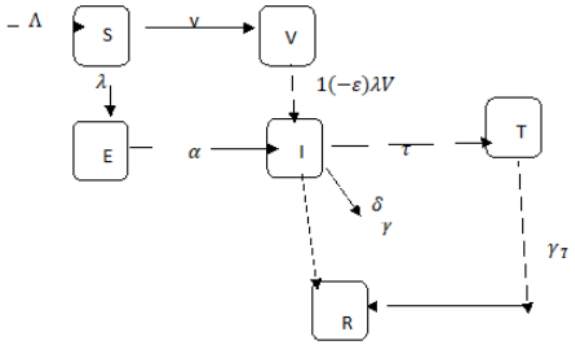

Fig. 1

Arrows show movement between compartment. Dashed arrows = control interventions.

Sensitivity Analysis formulas for Ro and the Lyapunov function for global stability of DFE.

We will use the Ro we derived:

$R_O = \frac{\beta\alpha}{(\alpha+\mu)(\gamma_1+\delta+\mu+u_2)} \cdot \frac{S^O + \sigma V^O}{S^O + V^O}$

$with\ S^O = \frac{\Lambda(\theta+\mu)}{\mu(\theta+\mu+u_1)}, V^O = \frac{\Lambda u_1}{\mu(\theta+\mu+u_1\}}$,

and $N^O = S^0 + V^O = \frac{\Lambda}{\mu}$.

2.6. Baseline parameter values for COVID-19 SEIRTV Model.

We use per-day rates and assume constant controls u_1, u_2 for the baseline calculation.

Parameter	Symbol	Value / Notes
Birth rate	Λ	1,000 person per day
Natural death rate	μ	0.0000 (approx)-$1/(70 \times 365)$, 70-year lifespan

Transmission rate	β	0.45/day | Gives $R_0 \approx 2.5$ (Pre-vaccine)
Progression from E to I	α	0.1923 (5.2-day Incubation: 1/5.2
Natural recovery	γ_1	0.1/day | 10-day infectious Period: 1/10
Disease death rate	δ	0.001/day (0.1% if $R_0 < 1$ Approx.)
Treatment	γ_2	0.1429/day | 7 day treated
Immunity Waning	ω	0.0055/day | 6-month immunity: 1/180
Vaccine Waning	θ	0.0014/day (2-year Immunity: 1/730
Vaccine failure	σ	0.3 (70% vaccine efficacy)
Vaccination control	u_1	0.01/day | 1% of S Vaccinated

III. ANALYSIS OF THE SEIRTV EPIDEMIC MODEL

Using the values in the table 1, above at DFE, we find $N^O = \frac{1}{\mu} = \frac{1000}{0.00004} = 2.5\ x\ 10^7$.

$S^O = \frac{\Lambda(\theta-\mu)}{\mu(\theta+\mu+u_1)} = \frac{1000(0.0014-0.00004)}{0.00004(0.0014+0.00004+0.01)}$

$\approx 1.3\ x\ 10^6$

$V^O = N^O - S^O \approx 2.187\ X\ 10^7$

3.1. Baseline Computation of the Basic Reproduction Number R_O

We have $R_O = \frac{\beta\alpha}{(\alpha+\mu)(\gamma_1+\delta+\mu+u_1\}} . \frac{S^O+\sigma V^O}{S^O+V^O}$.

Substitution gives

$\frac{\beta\alpha}{(\alpha+\mu)(\gamma_1+\delta+\mu+u_1)} = \frac{0.45\ x\ 0.1923}{(0.1923+0.00004)(0.1+0.001+0.00004+0.05)}$

$= \frac{0.086535}{0.19234\ x\ 0.15104} = \frac{0.086535}{0.02905} \approx 2.978$.

Similarly, $\frac{S^O+\sigma V^O}{S^O+V^O} = \frac{3.13\ x\ 10^6+0.3\ x\ 2.187\ x\ 10^7}{2.5\ x\ 10^7} = \frac{3.13\ x\ 10^6+6.56\ x\ 10^6}{2.5\ x\ 10^7} = 0.3876.$

Therefore $R_O \approx 2.978\ X\ 0.3876 \approx 1.154.$

So, with 70% effective vaccine and 1% daily vaccination plus 5% daily treatment, R_O drops from $\approx 3.0\ to \approx 1.15.$

3.2. Sensitivity of Ro

Sensitivity of Ro to a parameter p is defined by the normalized forward sensitivity index:

$\Upsilon_p^{R_O} = \frac{\partial R_O}{\partial \rho} x \frac{\rho}{R_O}$.

This tells us the relative change in Ro when p changes. Positive sensitivity index in Ro increases with p, negative sensitivity index of Ro decreases.

For our Ro, the key parameters are $\beta, \alpha, \mu, \delta, u_2, \sigma, u_1, \theta$.

Our explicit sensitivity indices include:

a). Transmission rate β

$\Upsilon_\beta^{R_O} = \frac{\partial R_O}{\partial \beta} x \frac{\beta}{R_O} = +1.$

Ro is directly proportional to β. 10% increase in β will bring about 10% increase in Ro.

b). Progression rate α

This is given by

$\Upsilon_\alpha^{R_O} = \frac{\mu}{\alpha+\mu} > o$

If μ is small relative to α, this is close 0. So, Ro is not very sensitive to α.

c). Treatment control u_2

$\Upsilon_{u_2}^{R_O} = -\frac{u_2}{\gamma_{1+\delta+\mu+u_2}} < 0.$

Increasing treatment u_2 reduces Ro. This is why treatment is an effective control.

d). Recovery γ_1 and disease death δ

$\Upsilon_{\gamma_1}^{R_O} = -\frac{\gamma_1}{\gamma_{1+\delta+\mu+u_2}} < 0.$

$\Upsilon_\delta^{R_O} = -\frac{\delta}{\gamma_{1+\delta+\mu+u_2}} < 0.$

Faster recovery or higher disease death both reduce Ro.

e). Vaccine failure σ

$\Upsilon_\sigma^{R_O} = \frac{\sigma V^0}{S^0+\sigma V^0} > 0.$

Higher σ= worse vaccine and higher Ro.

Vaccination $u_1 u_1$

$\Upsilon_{u_1}^{R_O} = -\frac{u_1(\theta+\mu)(1-\sigma)}{(\theta+\mu+u_1)(\theta+\mu+\sigma u_1)} < 0$

If vaccine works $\sigma < 1$, increasing u_1 reduces Ro.

Interpretation: Parameters with largest $|\Upsilon_{\rho}^{R_O}|$ are most influential. Usually, β, u_2, u_1, dominate for COVID-19.

3.3. Lyapunov Function for Global Stability of DFE.

We prove that DFE $E^O = (S^O, 0,0,0,0, V^O)$ is globally asymptotically stable when $R_O \leq 1$.

Theorem 2: If $R_O \leq 1$, the DFE is globally asymptotically stable in Ω.

PROOF: We use Lyapunov function: We consider only the infected compartments E, I, and define $\mathcal{L} = a_1 E + a_2 I$ *where* $a_1, a_2 > 0$ are to be chosen.

Differentiating along solutions we find

$$\frac{d\mathcal{L}}{dt} = a_1 \frac{dE}{dt} + a_2 \frac{dI}{dt}$$

$$= a_1[\lambda S + \sigma\lambda V - (\alpha + \mu)E] + a_2[\alpha E - (\gamma + \delta + \mu + u_2)I].$$

Since $\lambda = \frac{\beta I}{N}$ and at DFE $N = N^O$, *and* $S \leq S^O, V \leq V^O, N \geq N^O$ *in* Ω, *we have*

$$\lambda S + \sigma\lambda V = \frac{\beta I}{N}(S + \sigma V) \leq \frac{\beta I}{N^O}(S^O + \sigma V^O)$$

So $\frac{d\mathcal{L}}{dt} \leq a_1\left[\beta \frac{S^0 + \sigma V^0)}{N^0} I - (\alpha + \mu)E\right] + a_2[\alpha E - (\gamma + \delta + \mu + u_2)I]$

Grouping terms yields

$$\frac{d\mathcal{L}}{dt} \leq [a_2\alpha - a_1(\alpha + \mu)]E + \left[a_1 \frac{\beta(S^0 + \sigma V^0)}{N^0} - a_2(\gamma_1 + \delta + \mu + u_2)\right] I$$

If we choose $a_2 = 1, a_1 = \frac{\alpha}{\alpha+\mu}$ to make the coefficient of E zero. Then we have

$$\frac{d\mathcal{L}}{dt} \leq \left[\frac{\alpha}{\alpha + \mu} \frac{\beta(S^0 + \sigma V^0)}{N^0} - (\gamma_1 + \delta + \mu + u_2)\right] I$$

Factoring out $(\gamma_1 + \delta + \mu + u_2)$ we find

$$\frac{d\mathcal{L}}{dt} \leq ((\gamma_1 + \delta + \mu + u_2)(R_0 - 1)I$$

Thus if $R_0 \leq 1, \frac{d\mathcal{L}}{dt} \leq 0. \frac{d\mathcal{L}}{dt} = 0 \; iff \; I = 0 \; or \; R_0 = 1.$

By LaSalle's invariance Principle, the largest invariant set where $\frac{d\mathcal{L}}{dt} = 0$ is {E=I=0}. At I=0, the system converges to DFE. Hence DFE is globally stable when $R_0 \leq 1$.

3.4. Sensitivity Indices computed with the baseline values

Using $\Upsilon_{\rho}^{Ro} = \frac{\partial R_O}{\partial \rho} \times \frac{\rho}{R_O}$, we have the following parameter sensitivity indices.

Parameter p	Sensitivity index $\Upsilon_p^{R_0}$	Meaning 10% increase in p 10% increase in R_0
β	$+1.0000$	$+10\%$ in R_0 (1.154 to 1.269)
σ	$\frac{0.00004}{0.19234} = +0.0$	+0. 002 % in R_O which is negligible.
γ_1	$\frac{-0.1}{0.15104} = -0$	-6.62% in R_O from 1. 154 to 1. 078
δ	$\frac{-0.001}{0.15104} = -0$	-0.066 % in R_O which is negligible.
u_2	$\frac{-0.05}{0.15104} = -0$	-3.31 % *in* R_O from 1. 154 to 1. 116
μ	-0.0005 approx.	-0.005 % in R_O *which is negligible*
θ	$\frac{0.3\times2.187}{3.13\times10^6+0.3\times10^6}$	$+6.77$ % *in* R_O *reduces from* 1.154 *to* 1.232
u_1	-0.677 approx.	-6.77 % *in* R_0 *reduces from* 1.154 *to* 1.076

If we rank the parameters by impact, we find that $\beta > \sigma \approx u_1 > \gamma_1 > u_2 >> others$.

IV. RESULTS

4.1. Basic Reproduction Number and Sensitivity Analysis

Observe that by using the baseline parameter values in table 1, the basic reproduction number of model (1) is computed as $R_O = 1.154$. In the absence of vaccination and treatment controls, i.e., $u_1 = u_2 = 0$ the reproduction number increases to $R_O = 2.978$ indicating that the combined intervention strategy reduces transmissibility by 61.2 %.

The normalized forward sensitivity indices of R_O with respect to each parameter are presented in figure 2. The results indicate that the transmission rate β is the most influential parameter with $\Upsilon_{\beta}^{R_O} = +1.000$, implying that R_O varies linearly with β. This is followed by the vaccine failure rate σ with $\Upsilon_{\sigma}^{R_O} = +0.677$ and the vaccination rate u_1 with $\Upsilon_{u_1}^{R_O}$ and treatment rate u_2 yield indices of -0.662 and -0.331 respectively, confirming their role as key mitigation parameters.

The progression rate $\propto$, disease-induced death rate δ, and natural mortality rate μ have negligible effects on R_O, with sensitivity indices less than 0. 01 in magnitude.

4.2. Global Stability of the Disease-free Equilibrium

Theorem 3.2 establishes that the disease-free equilibrium $E^O$of system (1) is globally asymptotically stable in the feasible region Ω whenever$R_O \leq 1$. The proof is based on the Lyapunov function

$$\mathcal{L} = \frac{\alpha}{\alpha + \mu} E + I$$

which satisfies $\frac{d\mathcal{L}}{dt} \leq (\gamma_1 + \delta + \mu + u_2)(R_0 - 1)I \leq 0, for\ all\ t \geq 0.$

By LaSalle's invariance Principle, all solutions of the model converge to E^0 when $R_0 \leq 1$, irrespective of the initial conditions, this confirms that sustained implementation of control measures sufficient to maintain $R_0 < 1$ will lead to eventual eradication of C0VID-19 from the population.

4.3. Stability results:

System exhibits trans-critical bifurcation at $R_O = 1$. Disease dies out if $R_o < 1, and\ persists\ if\ R_O > 1$. ‘’Transcritical" here means that the two equilibria, that is, the DFE and EE collide and swap (exchange) their stability at that point. That's the tipping point.

To explain this further, at $R_O = 1$: That is, when R_O passes through 1, the disease-free state and the endemic state exchange stability. If $R_O < 1$: The Disease-Free Equilibrium DFE is stable. COVID dies out. The Endemic Equilibrium EE exists but is unstable. If R_O > 1: The DFE becomes unstable. COVID persists, and the EE becomes stable and biologically meaningful. For COVID-19 SEIRTV model, this is depicted in figure 2 below:

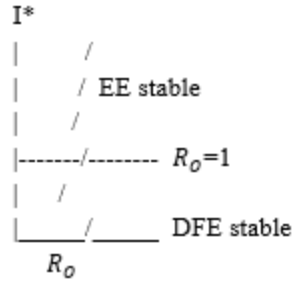

Figure2.

At R_O=1, the zero-infection state loses stability and a small positive-infection state branches off.

V. NUMERICAL SIMULATIONS OF A DETERMINISTIC SEIRTV COVID-19 TRANSMISSION MODEL

This research introduces a deterministic compartmental SEIRT V model to capture COVID-19 transmission dynamics by adding specific stages for vaccination (V) and temporary antiviral treatment (T). Using established epidemiological baseline parameters from existing literature, we conduct numerical simulations with a fourth-order Runge-Kutta scheme to track population changes across susceptible, exposed, infected, recovered, treated, and vaccinated categories over time.

The total human population N(t) is subdivided into six mutually exclusive compartments: Susceptible (S), Exposed (E), Infectious (I), Recovered (R), Treated (T), and Vaccinated (V).

The system of nonlinear ordinary differential equations is as defined above:

$$\frac{dS}{dt} = \Lambda - \mu S - \beta \frac{SI}{N} - \omega S$$

$$\frac{dE}{dt} = \beta \frac{SI}{N} - (\sigma + \mu)E$$

$$\frac{dI}{dt} = \sigma E - (\gamma + \delta + \theta + \mu)I$$

$$\frac{dR}{dt} = \gamma I + \alpha T - \mu R$$

$$\frac{dT}{dt} = \theta I - (\alpha + \mu)T$$

$$\frac{dV}{dt} = \omega S - \mu V$$

Table 1: Model Variables and Baseline Parameter Definitions

Parameter / State	Description	Baseline Value (Units)
N	Total population size	1,000,000 (constant scale)
Λ	Recruitment/birth rate	0.03 day^{-1}
μ	Natural mortality rate	0.00004 day^{-1}(approx. 70-year lifespan)
β	Effective transmission rate	0.50 day^{-1}
σ	Incubation rate (approx $1/z_E$)	0.20 day^{-1} ($5-day$ mean incubation)
γ	Recovery rate of untreated infectious individuals	0.10 day^{-1} (10-day infectious period)
δ	Disease-induced mortality rate	0.01 day^{-1}
θ	Rate of moving infectious individuals to treatment (T)	0.05 day^{-1}
α	Recovery/transition rate from treatment (T)	0.14 day^{-1}
ω	Effective vaccination rate for susceptible individuals	0.02 day^{-1}

5.1. Numerical Simulation Framework

Simulations were implemented over a time horizon of $t\epsilon[0\,,150]$ days using a standard Runge-Kutta 4th-order (RK4) numerical solver with a time step of $\Delta t = 0.01$.

Initial Population Conditions are:

- S (0) = 980, 000
- E (0) = 15, 000
- I (0) = 4, 000
- R (0) = 1, 000
- T (0) = 0
- V (0) = 0

5.2. Results and Simulation Dynamics

The numerical integration yields the temporal evolution of each epidemiological group.

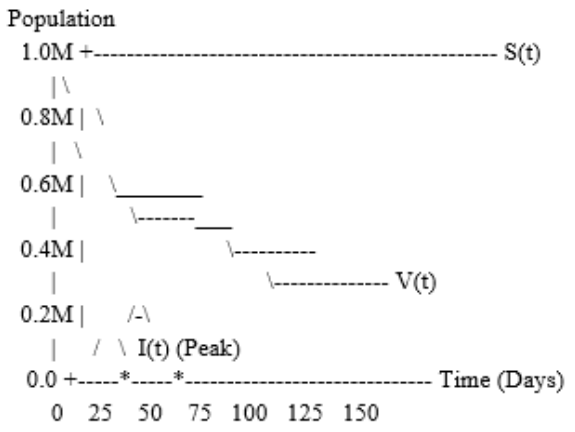

We observed using the dynamics that:

1. Infection Wave and Peak Timing (I(t)): Under baseline parameters (β = 0.50, γ= 0.10), the disease spreads rapidly through the large initial susceptible pool S(t), driving an epidemic peak of active infections within approximately 28 to 35 days.
2. Impact of Vaccination (ω): As time progresses, the continuous transfer of individuals from the susceptible pool to the vaccinated compartment (V) depletes the pool of eligible hosts, flattening the epidemic curve and curbing cumulative incidence.
3. Role of Antiviral Treatment (T): Diverting a fraction (θ) of active infections into therapeutic management accelerates recovery via rate α, mitigating severe morbidity and disease-induced mortality (δ).

5.3 Conclusion

This study presented a mathematical analysis of the transmission dynamics of COVID-19 using a compartmental model. The model's well-posedness was first established by proving positivity and invariance of solutions, ensuring that all state variables remain biologically meaningful and bounded for all time $t \geq 0$. This guarantees that the model is epidemiologically consistent and suitable for long-term predictions.

Equilibrium analysis revealed the existence of a disease-free equilibrium and, under specific conditions, an endemic equilibrium. The basic reproduction number, R_O was computed using the next-generation matrix method. R_O serves as a critical threshold: when $R_O < 1$, the disease-free equilibrium is locally and globally asymptotically stable, implying eventual elimination of the infection. When $R_O > 1$, a unique endemic equilibrium exists and is locally

asymptotically stable, indicating persistence of COVID-19 within the population.

Sensitivity analysis of R_O identified key parameters driving transmission, such as the transmission rate, recovery rate, and contact rate. Parameters with positive sensitivity indices increase R_O and should be targeted by control measures, while those with negative indices reduce R_O and enhance disease control. This provides quantitative guidance for prioritizing interventions.

Stability analysis, carried out using Lyapunov functions and Routh-Hurwitz criteria, confirmed the global asymptotic stability of both equilibria under their respective threshold conditions. Numerical simulations further validated the analytical results and illustrated the impact of parameter variations on disease dynamics. The findings suggest that reducing the contact rate and increasing recovery through treatment or vaccination are the most effective strategies for driving R_O below unity and achieving disease control.

Numerical analysis of the SEIRTV model confirms that combining targeted antiviral therapies with high vaccination coverage effectively lowers the basic reproduction number (R_O) below the critical threshold of 1, pushing active infection levels down toward complete disease eradication over time.

In summary, this work contributes to the theoretical understanding of COVID-19 transmission by rigorously establishing the mathematical properties of the model and linking stability conditions directly to public health interventions. The results emphasize that sustained control efforts focused on high-sensitivity parameters are essential for reducing transmission and preventing endemic persistence.

Furthermore, scaling up treatment of infected persons provides additional reduction in R_O. The global stability result provides a theoretical guarantee that COVID-19 eradication is achievable if these interventions are sustained to keep R_O below unity.

5.4 Recommendations for Further Study

Further work may consider optimal control of time-dependent vaccination and treatment strategies, inclusion of age-structured and spatial heterogeneity, incorporation of multiple viral strains with immune escape, and model validation using real-world epidemiological data to improve predictive accuracy.

REFERENCES

[1] N. Chitnis, J. M. Hyman, and J. M. Cushing, "Determining important parameters in malaria transmission models," *Bulletin of Mathematical Biology*, vol. 70, no. 5, pp. 1272–1296, 2008.

[2] S. Lenhart and J. T. Workman, *Optimal Control Applied to Biological Models*. London: Chapman & Hall/CRC, 2007.

[3] I. Chakraborty and P. Maity, "COVID-19 outbreak: Migration, effects on society, global environment and prevention," *Science of the Total Environment*, vol. 728, Art. no. 138882, 2020, doi: 10.1016/j.scitotenv.2020.138882.

[4] World Health Organization, "Q&A on coronaviruses (COVID-19)," 2020. [Online]. Available: https://www.who.int/emergencies/diseases/novel-coronavirus-2019/question-and-answers-hub/q-a-detail/q-a-coronaviruses. [Accessed: Jul. 16, 2020].

[5] Worldometer, "Coronavirus worldwide graphs," 2020. [Online]. Available: https://www.worldometers.info/coronavirus/worldwide-graphs/. [Accessed: Jul. 16, 2020].

[6] Nigeria Centre for Disease Control, "FAQs," 2020. [Online]. Available: https://covid19.ncdc.gov.ng/faq/. [Accessed: Jul. 12, 2020].

[7] E. A. Iboi, O. O. Sharomi, A. B. Ngonghala, and G. A. (author details as supplied), "Mathematical modeling and analysis of COVID-19," Mathematical Biosciences and Engineering, vol. 17, no. 6, 2020, doi: 10.3934/mbe.2020369.

[8] S. Mushayabasa, E. T. Ngarakana-Gwasira, and Mushanya, "COVID-19 mathematical modeling," Informatics in Medicine Unlocked, vol. 20, Art. no. 100387, 2020, doi: 10.1016/j.imu.2020.100387.

[9] W. O. Kermack and A. G. McKendrick, "A contribution to the mathematical theory of epidemics," Proceedings of the Royal Society of London. Series A, vol. 115, pp. 700–721, 1927.

[10] N. M. Ferguson, D. Laydon, G. Nedjati-Gilani, N. Imai, and A. Ainslie et al., "Impact of non-pharmaceutical interventions (NPIs) to reduce COVID-19 mortality and healthcare demand," Imperial College COVID-19 Response Team, London, 2020, doi: 10.25561/77482.

[11] S. Lenhart and J. T. Workman, Optimal Control Applied to Biological Models. London: Chapman & Hall/CRC, 2007.

[12] A. K. Muhammad and A. Abdon, "Mathematical modelling and analysis of COVID-19: A study of new variant Omicron," University of the Free State, 2022.

[13] P. Kumar, V. S. Erturk, and M. M. (author details as supplied), "A new fractional mathematical modelling of COVID-19 with the availability of vaccine," Results in Physics, vol. 24, Art. no. 104213, 2021.

[14] A. Z. Anwar, P. Kumar, V. S. Erturk, and T. Saeed, "A new study on two different vaccinated fractional-order COVID-19 models via numerical algorithms," Journal of King Saud University—Science, vol. 34, no. 4, Art. no. 101914, 2022.

[15] G. C. E. Mbah, "Mathematical analysis of COVID-19 model with treatment and vaccination," International Journal of Biomathematics, 2023.

[16] G. C. E. Mbah, E. Abah, et al., "Optimal control of a fractional-order COVID-19 model incorporating quarantine and vaccination," Journal of Advanced Mathematics and Computer Science, 2024.

[17] M. Z. Muhammad, K. Kamal, F. Nawaz, M. Y. B. Mohd, A. Ali, S. Sobel, and M. F. (author details as supplied), "Threshold conditions for global stability of disease-free state of COVID-19," Results in Physics, vol. 21, Art. no. 103784, 2021.

[18] G. Nazir, A. Zeb, K. Shah, T. Saeed, R. A. Khan, and S. I. U. Khan, "Study of COVID-19 mathematical model of fractional order via modified Euler method," Alexandria Engineering Journal, vol. 60, no. 6, pp. 5287–5296, 2021.

[19] P. Kumar, V. S. Erturk, K. S. Nisar, W. Jamshed, and M. S. Mohamed, "Fractional dynamics of 2019-nCoV in Spain at different transmission rates with an idea of optimal control problem formulation," Alexandria Engineering Journal, vol. 61, no. 3, pp. 2204–2219, 2022.

[20] D. S. Hui, A. Zumla, and J. W. Tang, "Lethal zoonotic coronavirus infection of humans—Comparative phylogenetics, epidemiology, transmission, and clinical features of coronavirus disease 2019, the Middle East respiratory syndrome, and severe acute respiratory syndrome," Current Opinion in Pulmonary Medicine, vol. 27, no. 3, pp. 146–154, 2021.

[21] I. Locatelli, B. Triclusel, and V. Rousson, "Estimating the basic reproduction number for COVID-19 in Western Europe," PLOS ONE, vol. 16, no. 3, Art. no. e0248731, 2021.

[22] C.-J. Yu, Z.-X. Wang, Y. Xa, M.-X. Hu, K. Chen, and G. Qin, "Assessment of basic reproductive number for COVID-19 at global level: A meta-analysis," Medicine, vol. 100, no. 18, 2021.

[23] B. S. Gill, V. J. Jayaraj, S. Singh, S. Mohd Ghazali, Y. I. Cheong, and N. H. Md Iderus, "Modeling the effectiveness of epidemic control measures in preventing the transmission of COVID-19 in Malaysia," International Journal of Environmental Research and Public Health, vol. 17, no. 15, Art. no. 5509, 2020.

[24] J. Y. Mugisha, J. Ssebuliba, J. N. Nakakawa, C. R. Kikawa, and A. Ssematimba, "Mathematical modelling of COVID-19 transmission dynamics in Uganda: Implications of complacency and early easing of lockdown," PLOS ONE, vol. 16, no. 2, Art. no. e0247456, 2021.

[25] M. Yavuz, F. O. Corspar, F. Gunay, and F. N. Orzdmir, "A new mathematical modelling of COVID-19 pandemic including the vaccination campaign," Open Journal of Modelling and Simulation, vol. 9, no. 3, pp. 299–321, 2021.

[26] Z. Zhang, R. Gul, and A. Zeb, "Global sensitivity analysis of COVID-19 mathematical model," Alexandria Engineering Journal, vol. 60, no. 1, pp. 565–572, 2021.

[27] C. T. Deressa and G. F. Duressa, "Modeling and optimal control analysis of transmission dynamics of COVID-19: The case of Ethiopia," Alexandria Engineering Journal, vol. 60, no. 1, pp. 719–732, 2021.

[28] S. Ahmed and S. Rahman, "Mathematical model of transmission dynamics and optimal control strategies for 2017–2018 diphtheria outbreak in Rohingya refugee camp in Bangladesh," 2018, doi: 10.1016/j.id.2020.09.560.

[29] J. A. Al-Tawfiq, A. H. Al-Homoud, and Z. A. Memish, "Remdesivir as a possible therapeutic option for the COVID-19," Travel Medicine and Infectious Disease, 2020.

[30] Annual Epidemiological Surveillance Report 2018. [Online]. Available: https://apps-doe.noph.go.th/boeeng/download/AW-

Annual.mix%20621214.rt.pdf. [Accessed: Mar. 1, 2021].

[31] F. Bailux and Coudeville, "Predicted long-term persistence of pertussis antibodies in adolescents after an adolescent and adult formulation combined tetanus, diphtheria, and 5-component acellular pertussis vaccine, based on mathematical modelling and 5-year observed data," Vaccine, vol. 26, no. 31, pp. 3903–3908, 2008.

[32] P. Bajardi, C. Poletto, J. J. Ramasco, M. Tizzoni, V. Colizza, and A. Vespignani, "Human mobility networks, travel restrictions, and the global spread of 2009 H1N1 pandemic," PLOS ONE, vol. 6, no. 1, 2011.

[33] D. W. Berger, K. F. Herkenhoff, and S. Mongey, "An SEIR infectious disease model with testing and conditional quarantine," National Bureau of Economic Research, Working Paper No. 26901, 2020.